Metalorganic vapor-phase epitaxial growth and photoluminescent properties of $Zn_{1-x}Mg_xO(0 \leqslant x \leqslant 0.49)$ thin films

W. I. Park, Gyu-Chul Yi,[a] and H. M. Jang
Department of Materials Science and Engineering, Pohang University of Science and Technology (POSTECH), Pohang 790-784, Korea

(Received 16 April 2001; accepted for publication 23 July 2001)

High-quality $Zn_{1-x}Mg_xO(0.00 \leqslant x \leqslant 0.49)$ thin films were epitaxially grown at 500–650 °C on $Al_2O_3(00 \cdot 1)$ substrates using metalorganic vapor-phase epitaxy. By increasing the Mg content in the films up to 49 at. %, the *c*-axis constant of the films decreased from 5.21 to 5.14 Å and no significant phase separation was observed as determined by x-ray diffraction measurements. Furthermore, the near-band-edge emission peak position showed blueshifts of 100, 440, and 685 meV at Mg content levels of 9, 29, and 49 at. %, respectively. Photoluminescent properties of the alloy films are also discussed. © *2001 American Institute of Physics.* [DOI: 10.1063/1.1405811]

ZnO, a wide-gap semiconductor oxide, has attracted considerable attention due to its large exciton binding energy (~60 meV) and bond strength, which might make reliable high-efficiency photonic devices based on ZnO.[1–3] Moreover, as reported by Othomo *et al.*,[4] the fundamental band-gap energy of this material increases from 3.3 to 4.0 eV by alloying ZnO with MgO, depending on the Mg content, which might be practically used for fabrications of $ZnO/Zn_{1-x}Mg_xO$ heterostructure light emitters as well as ultraviolet photodetectors. In the low-dimensional double heterostructure, the modified density of states confines both excitons and photons, making the stimulated emission process more efficient.[5]

Recently, it has been reported that $Zn_{1-x}Mg_xO$ was grown with maximum Mg incorporation up to 36 at. % without phase separation and that the room-temperature luminescence energy in this film blueshifted from 3.3 to 4.0 eV.[6] Since a $Zn_{1-x}Mg_xO$ containing MgO over 4 at. % is in a thermodynamically metastable state,[7] this result indicates that the solubility limit of Mg in ZnO depends on growth mechanisms as well as growth conditions. However, current research on the growth of $Zn_{1-x}Mg_xO$ is restricted to pulsed-laser deposition (PLD) and molecular-beam epitaxy (MBE). Despite the epitaxial growth of high-quality ZnO and related alloys using the methods, they might have disadvantages in mass production, due to high cost and low throughput. In this research, we demonstrate that metalorganic vapor-phase epitaxy (MOVPE), which has great advantages in terms of large-area deposition and atomic composition control feasibility, is an excellent technique for the epitaxial growth of high-quality $Zn_{1-x}Mg_xO$ films.

$Zn_{1-x}Mg_xO(0.0 \leqslant x \leqslant 1.0)$ films were grown on $Al_2O_3(00.1)$ substrates using a horizontal-type MOVPE system. For film growth, diethylzinc (DEZn), *bis*-cyclopentadienyl-Mg (cp_2Mg), and oxygen were employed as the reactants with argon as the carrier gas. Details of ZnO film growth have previously been reported.[3] Typical cp_2Mg flow rates were in the range of 0–50 sccm at the bubbler temperature of 30–40 °C. Before ZnMgO film growth, thin ZnO buffer layers were initially grown, which significantly improved the crystallinity of $Zn_{1-x}Mg_xO$ films. Film thicknesses were in the range of 0.3–0.7 μm as determined using surface profilometry.

The crystal structure, crystallinity, and lattice parameters of $Zn_{1-x}Mg_xO$ films were investigated by x-ray diffraction (XRD) measurements using a rotating anode-type x-ray diffractometer. Although film compositions can be estimated from lattice parameters changed by Mg incorporation, they were more accurately determined by both energy-dispersive x-ray analysis and inductively coupled plasma mass spectrometry.

Photoluminescence (PL) measurements were performed for optical characterization of the films. As an excitation source for the PL measurements of $Zn_{1-x}Mg_xO$ films, a He–Cd laser (325 nm) was employed for $x \leqslant 0.18$ and the fourth harmonics (266 nm) of a Nd:YAG laser for $x \geqslant 0.20$. Details of the PL measurements have been previously reported.[8]

The crystal structure and orientation of the as-grown films were investigated, measuring θ–2θ scans of XRD. As shown in Fig. 1(a), up to $x = 0.49$ in $Zn_{1-x}Mg_xO$ films, θ–2θ scan data exhibited only $Zn_{1-x}Mg_xO(00 \cdot 2)$ peaks at 34.36°–35.01°, depending on the Mg content. The observation of only $ZnMgO(00 \cdot l)$ peaks indicates that single-phase $Zn_{1-x}Mg_xO(0.0 \leqslant x \leqslant 0.49)$ films were grown without any significant formation of a separated MgO phase. However, for the higher-Mg content of 75 at. %, a MgO(111) peak was also observed, clearly indicating phase separation between ZnO and MgO. In addition, the MgO peak intensity gradually increased but the $ZnMgO(00 \cdot 2)$ peak decreased by increasing the cp_2Mg flow rate.

In general, $Zn_{1-x}Mg_xO$ with a high concentration of Mg over 4 at. % is not thermodynamically stable. However, MOVPE demonstrates growth of high-quality, single-phase $Zn_{1-x}Mg_xO$ with Mg containing up to 49 at. %. Similar behavior has previously been observed: other growth techniques, MBE and PLD have also shown the incorporation of the high-Mg concentration, 33–36 at. %.[4,6,9] Nevertheless, the enhancement in the solubility limit of MOVPE-grown ZnMgO might be explained in terms of the low-growth tem-

[a]Electronic mail: gcyi@postech.ac.kr

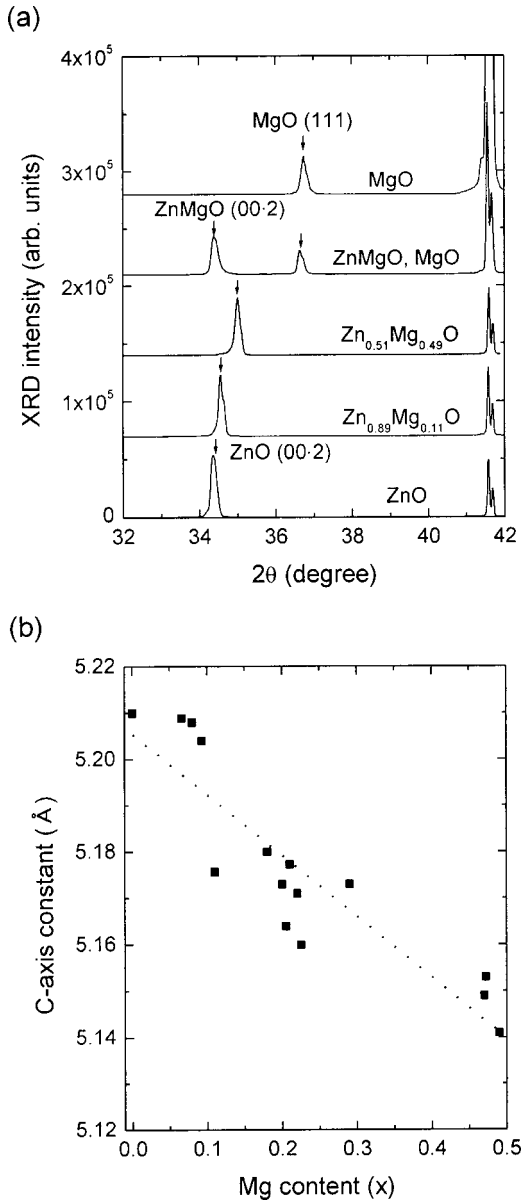

FIG. 1. (a) XRD θ–2θ scan results of $Zn_{1-x}Mg_xO$ ($0.0 \leqslant x \leqslant 1$) and (b) Mg concentration dependence of the c-axis constant of $Zn_{1-x}Mg_xO$ ($0.0 \leqslant x \leqslant 0.49$) films.

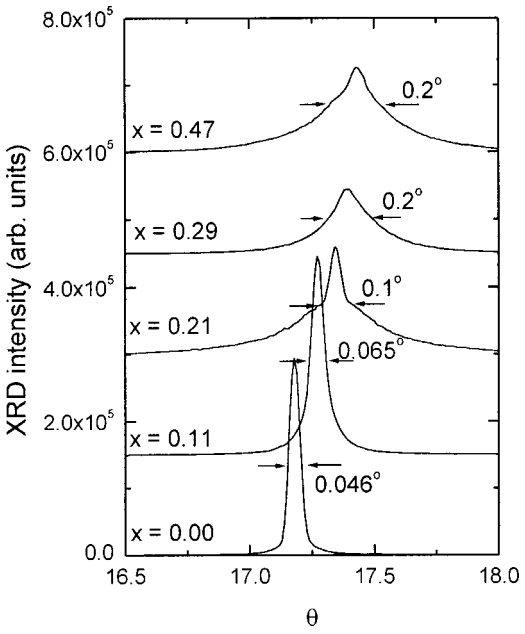

FIG. 2. Typical x-ray rocking curves of ZnMgO films. FWHM values of the $Zn_{1-x}Mg_xO$ films at $x = 0.0$, 0.11, 0.21, 0.29, and 0.47 are 0.046°, 0.065°, 0.1°, 0.2°, and 0.2°, respectively.

perature or chemical reactions employed in this MOVPE growth. When the films are grown at a low temperature employing chemical reactions between precursors, the chemical reaction allows epitaxial growth of single-phase ZnMgO alloys as long as the thermal energy is too low to form the second phase of MgO.

There is further unequivocal evidence for Mg incorporation into ZnO: the c-axis lattice constant of the $Zn_{1-x}Mg_xO$ films decreased by increasing the Mg content. As shown in Fig. 1(a), the $Zn_{1-x}Mg_xO(00\cdot2)$ XRD peaks were shifted to higher angles, indicating the decreases in the c-axis lattice constant of the films due to Mg incorporation. From the $(00\cdot l)$ diffraction peaks, c-axis lattice constants were determined by plotting their values as a function of $\cos^2\theta/\sin\theta$ and extrapolating to $\theta = 90°$.[10] As plotted in Fig. 1(b), the c-axis lattice constant of $Zn_{1-x}Mg_xO$ for $x = 0.49$ decreased by 1.34%, comparable to the 0.9% decrease for MBE-grown $Zn_{1-x}Mg_xO$ ($x = 0.33$).[9] Compared with similar ternary $Al_xGa_{1-x}N$ ($x = 0.4$), which shows a decrease in the lattice constant by ~2%,[11] $Zn_{1-x}Mg_xO$ alloys show a relatively smaller change in the lattice constant. This originates presumably from the similarity of the ionic radius between Zn^{2+}(0.83 Å) and Mg^{2+}(0.78 Å),[12] which can facilitate heteroepitaxial growth of $ZnO/Zn_{1-x}Mg_xO$ superlattices.

The effect of Mg incorporation on the crystallinity of $Zn_{1-x}Mg_xO$ films was also investigated measuring the XRD rocking curves of $Zn_{1-x}Mg_xO$ films. For this investigation the films were grown at the same growth condition except the cp_2Mg flow rate. As shown in Fig. 2, the $Zn_{1-x}Mg_xO$ film with a low-Mg content (x) of 0.11 shows the narrow full width at half maximum (FWHM) value of 0.065°, which is comparable to that of pure ZnO, 0.046°. However, for the $Zn_{0.79}Mg_{0.21}O$ film, the rocking curve shows the composition of two components showing FWHM values of 0.07° and 0.2°–0.3°. Similar to the case of ZnO films,[13] the broad component results presumably from three-dimensional islands nucleated on two-dimensional layers. With the further increase of Mg content, the broad component gradually became dominant. The deterioration in crystallinity of highly Mg-incorporated films might be due to strain induced from the occupation of Mg^{2+} ions at Zn^{2+} sites or increases in the film growth rates. Meanwhile, for ZnMgO films grown at low-growth rates, the broad component in the rocking curves was not observed and the FWHM values of $Zn_{1-x}Mg_xO$ films were as narrow as 0.07°.

Figure 3(a) shows typical photoluminescence spectra of the $Zn_{1-x}Mg_xO$ ($0.0 \leqslant x \leqslant 0.49$) films. From the PL spectra of the ZnO films, the dominant emission peak was observed at 3.364 eV with a FWHM of 7 meV, which is attributed to the excitons (I_2) bound to neutral donors.[3,14] However, the band-gap energy of $Zn_{1-x}Mg_xO$ depended on the Mg content, which results in a blueshift of the band-edge emission peak, as indicated by the dotted line. For $Zn_{1-x}Mg_xO$ films at $x = 0.09$, 0.29, and 0.49, the low-temperature NBE emis-

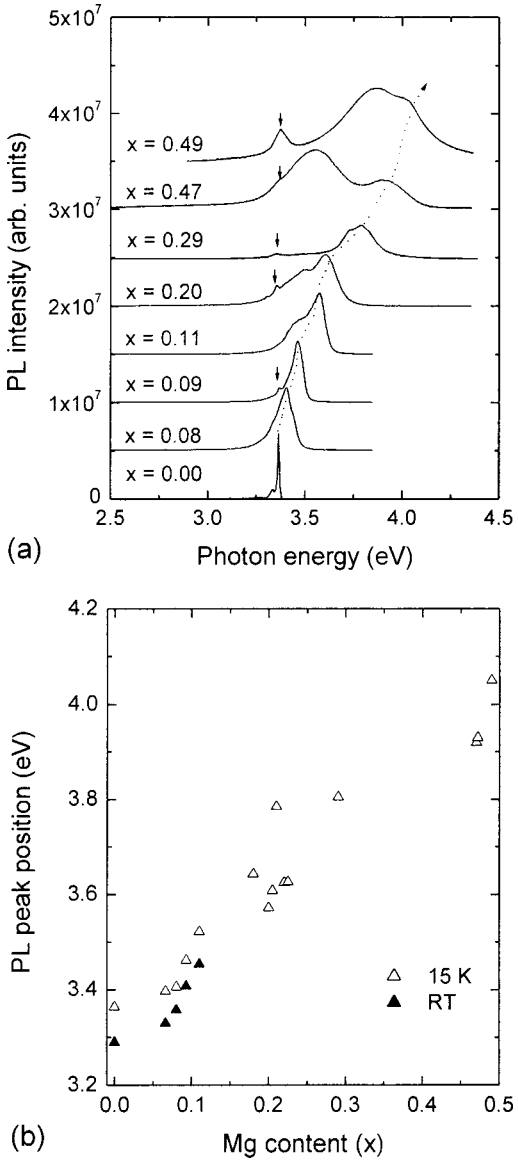

FIG. 3. (a) PL spectra of $Zn_{1-x}Mg_xO$ ($0.0 \leqslant x \leqslant 0.49$) films measured at 15 K and (b) Mg content dependence on NBE emission peak position at 15 K (△) and room temperature (▲).

sion peaks appeared at 3.462, 3.805, and 4.05 eV, respectively. For numerous x values between 0.0 and 0.49, the Mg content dependence on the NBE emission peak positions at 15 K (△) and room temperature (▲) is shown in Fig. 3(b). The blueshift was as large as 685 meV for $Zn_{0.51}Mg_{0.49}O$. Meanwhile, considering a large Stokes' shift in wide-band-gap semiconductors, the band gap of $Zn_{1-x}Mg_xO$ ($x = 0.49$) is estimated to be 4.3 eV with the simple assumption that the Stokes' shift exhibits a linear dependence on emission energy.[4,15,16]

Alloy broadening resulting in the Stokes' shift is commonly observed in alloy semiconductors.[15–17] The increase in the FWHM values of emission peaks by increasing Mg content (x) results presumably from the fluctuations in alloy composition, where localized excitons experience a different Coulomb potential. However, compared with other III–V alloy semiconductors, $Zn_{1-x}Mg_xO$ exhibits somewhat larger broadening parameters, which can be explained by the fact that excitons in $Zn_{1-x}Mg_xO$ have a small value of its Bohr radius and are, therefore, largely affected by local (atomic-scale) fluctuations of Mg content.[4]

It is noted that the weak emission peaks at 3.36 eV were also observed as indicated by arrows in Fig. 3(a), which results presumably from the bound excitons in the ZnO buffer layer. This is supported by the fact that the PL peak at 3.36 eV was not observed for $Zn_{1-x}Mg_xO$ thin films grown directly on sapphire substrates.

In conclusion, MOVPE was employed to grow high-quality $Zn_{1-x}Mg_xO$ epitaxial films up to $x = 0.49$. The c-axis lattice constants of the $Zn_{1-x}Mg_xO$ films decreased with increasing the Mg content. Due to the Mg incorporation, furthermore, the NBE emission peak of the films was blueshifted from 3.364 eV for $x = 0.0$ to 4.05 eV for $x = 0.49$.

This research was sponsored by the KISTEP through the National Research Laboratory program, the Brain Korea 21 project, and the POSTECH BSRI Special Fund-2001.

[1] D. M. Bagnall, Y. F. Chen, Z. Zhu, T. Yao, S. Koyama, M. Y. Shen, and T. Goto, Appl. Phys. Lett. **70**, 2230 (1997).
[2] Z. K. Tang, G. K. L. Wong, P. Yu, M. Kawasaki, A. Ohtomo, H. Koinuma, and Y. Segawa, Appl. Phys. Lett. **72**, 3270 (1998).
[3] W. I. Park, S.-J. An, G.-C. Yi, and H. M. Jang, J. Mater. Res. **16**, 1358 (2001).
[4] A. Ohtomo, M. Kawasaki, T. Koida, K. Masubuchi, H. Koinuma, Y. Sakurai, Y. Yoshida, T. Yasuda, and Y. Segawa, Appl. Phys. Lett. **72**, 2466 (1998).
[5] A. Ohtomo, K. Tamura, M. Kawasaki, T. Makino, Y. Segawa, Z. K. Tang, G. K. L. Wong, Y. Matsumoto, and H. Koinuma, Appl. Phys. Lett. **77**, 2204 (2000); H. D. Sun, T. Makino, N. T. Tuan, Y. Segawa, Z. K. Tang, G. K. L. Wong, M. Kawasaki, A. Ohtomo, K. Tamura, and H. Koinuma, *ibid.* **77**, 4250 (2000).
[6] A. K. Sharma, J. Narayan, J. F. Muth, C. W. Teng, C. Jin, A. Kvit, R. M. Kolbas, and O. W. Holland, Appl. Phys. Lett. **75**, 3327 (1999).
[7] E. R. Segnit and A. E. Holland, J. Am. Ceram. Soc. **48**, 412 (1965).
[8] W. I. Park and G.-C. Yi, J. Electron. Mater. (to be published).
[9] A. Ohtomo, M. Kawasaki, Y. Sakurai, I. Ohkubo, R. Shiroki, Y. Yoshida, T. Yasuda, Y. Segawa, and H. Koinuma, Mater. Sci. Eng., B **56**, 263 (1998).
[10] B. D. Cullity, *Elements of X-Ray Diffraction* (Addison-Wesley, Reading, MA, 1978).
[11] S. Yashida, S. Misawa, and S. Gonda, J. Appl. Phys. **53**, 6844 (1982).
[12] R. A. Flinn and P. K. Trojan, *Engineering Materials and Their Applications* (Houghton Mifflin, Boston, MA, 1975).
[13] S. I. Park, T. S. Cho, S. J. Doh, J. L. Lee, and J. H. Je, Appl. Phys. Lett. **77**, 349 (2000).
[14] D. C. Look, D. C. Reynolds, J. R. Sizelove, R. L. Jones, C. W. Litton, G. Cantwell, and W. C. Harsch, Solid State Commun. **105**, 399 (1998).
[15] R. W. Martin, P. G. Middleton, K. P. O'Donnell, and W. Van der Stricht, Appl. Phys. Lett. **74**, 263 (1999).
[16] K. P. O'Donnell, R. W. Martin, and P. G. Middleton, Phys. Rev. Lett. **82**, 237 (1999).
[17] S. Chichibu, T. Azuhata, T. Sota, and S. Nakamura, Appl. Phys. Lett. **69**, 4188 (1996).